Tien-Szu Wang[1]
Shang-Hao Liu[2]
Yu-Chi Lin[2]
Ying-Cyuan Chen[2]
Chi-Min Shu[2,3]

[1]National Yunlin University of Science and Technology (YunTech), Graduate School of Engineering Science and Technology, Yunlin, Taiwan, ROC.

[2]YunTech, Department of Safety, Health, and Environmental Engineering, Yunlin, Taiwan, ROC.

[3]China Medical University, Department of Occupational Safety and Health, Taichung, Taiwan, ROC.

Supporting Information available online

Green Process of Propylene Oxide Reaction for Thermal Hazard Assessment by Differential Scanning Calorimetry and Simulation

In addition to polypropylene, acrylonitrile, and carbonyl alcohol, propylene oxide is the fourth major derivative among propylene derivatives and one of the important basic organic chemicals. A thermal stability test of catalyst, methanol, and hydrogen peroxide (H_2O_2) was conducted via differential scanning calorimetry (DSC). Propylene epoxidation with H_2O_2 over catalyst, methanol, and propylene evenly mixed by specific pressure was carried out, and then the runaway reaction under adiabatic conditions was further simulated by the vent sizing package 2 (VSP2) to measure temperature and pressure data with respect to time of the runaway excursion. Finally, the apparent activation energy of H_2O_2 and propylene oxide reaction was obtained via temperature variation equation to evaluate the degree of potential hazard in industry.

Keywords: Differential scanning calorimetry, Hydrogen peroxide, Propylene oxide, Runaway reaction, Simulation

Received: February 21, 2014; *revised:* October 16, 2014; *accepted:* December 12, 2014

DOI: 10.1002/ceat.201400117

1 Introduction

The vigorous progress of the semiconductor industry and the transformation of the traditional petrochemical industry created enormous business opportunities. The rapid development of related materials and chemicals encouraged this transformation of traditional industries, such as high-purity chemicals and application patterns. Hydrogen peroxide (H_2O_2) is widely used in oxidizing or bleaching agents required in industrial production. In particular, high-purity H_2O_2 solution mixed with ammonium hydroxide (NH_4OH), sulfuric acid (H_2SO_4), and hydrochloric acid (HCl) in different proportions is an essential factor influencing the improvement of the wet cleaning technologies for semiconductors [1].

However, H_2O_2 is a strong oxidant with serious fire and explosion risks. When the solution concentration is more than 65 wt %, a spontaneous reaction can be readily generated. Moreover, when the solution concentration is more than 90 wt % and added with a catalyst or cross-linking agent, a swift decomposition can be caused more easily, resulting in high heat release rate, followed by runaway, fire, and even explosion hazard [2–4]. Therefore, a prudent assessment of the use of H_2O_2 is required. An earlier study found that the H_2O_2-titanium-silicon molecule is an excellent catalyst for olefin epoxidation [5, 6]. Concerning the current economic climate under green technology, one can substitute propylene epoxidation for propylene oxide [7]. The titanium-silicon molecule plays a crucial role as a catalyst in propylene epoxidation. The products of the green process, H_2O_2 to propylene oxide (HPPO), are merely propylene and water without by-products and derivatives which could pollute the environment (Fig. 1).

In the present experiment, the propylene epoxidation with 35 wt % H_2O_2 over catalyst, methanol (MeOH), and propylene were evenly mixed by specific pressure. Then, a thermal stability test was conducted using differential scanning calorimetry (DSC) to obtain the thermokinetic parameters, including exothermic onset temperature (T_0)[1)], exothermic peak temperature (T_p), and heat of decomposition (ΔH_d). The runaway reaction under adiabatic conditions, in turn, was simulated using vent sizing package 2 (VSP2) to determine temperature (T) and pressure (P) with respect to time (t) during the process as well as the thermal stability data in the thermal runaway reaction,

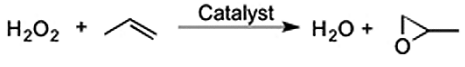

Figure 1. Propylene epoxidation with H_2O_2 over catalyst [14–16.]

Correspondence: Prof. Chi-Min Shu (hucm@yuntech.edu.tw), Department of Safety, Health, and Environmental Engineering, YunTech, 123, University Rd., Sec. 3, Douliou, Yunlin 64002, Taiwan, ROC.

1) List of symbols at the end of the paper.

including maximum temperature (T_{max}), maximum pressure (P_{max}), maximum pressure rise ($(dP\,dt^{-1})_{max}$), and maximum temperature rise ($(dT/dt)_{max}$). The standard experimental method for measuring the thermal stability of reaction in the manufacturing process was adopted to evaluate the thermal stability parameters for the design of the safer process conditions, to assess all kinds of related risks, and to establish the risk assessment techniques of the new process.

2 Experimental

2.1 Samples

H_2O_2 of 35 wt % and MeOH of 99 wt %, two limpid liquids, were purchased from Alfa Aesar and Aldrich, respectively. The catalyst as a white crystalline solid substance and propylene as liquid phase filled in a steel cylinder were provided from China Petrochemical Development Corp. (CPDC). H_2O_2 was stored in a refrigerator at 4 °C. Experimental techniques, such as preliminary estimate, DSC, TAM III, and VSP2 were proposed previously [8–13].

2.2 Methods

2.2.1 Propylene Oxide Reaction via H_2O_2

To improve production efficiency and process simplification, H_2O_2 was employed to produce HPPO via direct oxidation, i.e., H_2O_2 to HPPO, with reactants including propylene, MeOH, a titanium silicalite catalyst, and H_2O_2 as oxidant under the operating temperatures and pressures [14–16]. In the HPPO process, propylene can be gradually converted to HPPO under the above condition, and the main by-product is water, which may more effectively reduce the problem of subsequent contamination during the process. In view of the above mentioned facts, it not only overcomes the high pollution of chlorohydrin and the equipment corrosion problems, but also solves the problem of oxidation for styrene. Moreover, it has additional advantages such as short process pathway and lower equipment cost [17]. For these reasons, the procedure of propylene epoxide reaction is called green technology.

2.2.2 Dynamic Test

Experimental analysis was performed using the Mettler DSC821[e] and the analysis software STAR[e] [18]. DSC was applied for the preliminary thermal analysis of the substance to acquire the data for the exothermic curve and released heat as well as thermal behaviors. In the DSC test, H_2O_2 was placed in a gold crucible. The heating rate was set as 4 °C min^{-1} and the heating range was between 30 °C and 300 °C.

2.2.3 Adiabatic Test

VSP2, fabricated by Fauske & Associates, LLC [19], was used to measure the adiabatic state of the temperature and pressure with respect to time for reactants' changes in the heat-wait-search model [20, 21]. The test cell (Fauske & Associates, LLC) has a low thermal inertia factor (Φ) of about 1.05 to 1.32. Before the test, the thermocouple was tested in which the distance was around 5 mm between the bottom after cutting the test cell. In this experiment, although only 5.0 ± 0.1 g for 65 wt % H_2O_2 and 11 ± 0.1 g for HPPO reaction as listed in Tab. 3 were used, the thermocouple could still be immerged into the samples without any problems of temperature and pressure behaviors during 3–5 times testing for repeatability.

Here, MeOH, catalyst as a white powder, 35 wt % H_2O_2, and propylene were used. H_2O_2 was injected with a high-pressure syringe into the evenly mixed catalyst, MeOH, and propylene, and then a runaway reaction at 40 °C was simulated by means of VSP2. To solve the variation of system pressure, propylene was then deliberately injected several times to maintain the pressure at 28 psig, which was the minimum set pressure of the reaction condition from CPDC [17].

3 Results and Discussion

3.1 DSC Test Results: Inherent Hazard Analyses

Concentrations of 3, 10, 20, 30, and 35 wt % H_2O_2 were studied using DSC821[e] with differential scanning analysis function to determine the thermal stability of H_2O_2 and the exothermic phenomenon of the thermal decomposition reaction. To estimate the chemical kinetic parameters of H_2O_2, the thermal power profiles were measured in dynamic mode. As illustrated in Fig. 2, H_2O_2 concentrations between 3 and 35 wt % generated different exothermic reactions after heating, with heating ranging between 30 °C and 300 °C.

According to the exothermic peak temperatures listed in Tab. 1, T_0 of 35 wt % H_2O_2 was about 50 °C, ΔH_d was about 805.4 J g^{-1}, and T_p was about 77 °C. For the other different concentrations of H_2O_2 (3–30 wt %), T_0 was found to be 75, 67, 58,

Table 1. Experimental results of various concentrations of H_2O_2 via DSC test at 4 °C min^{-1}.

	Reactant		T_0[°C]	T_p[°C]	ΔH_d[J g^{-1}]
Substance	Mass [%]	Mass [mg]			
H_2O_2	3	5.0	75	85	58.6
	10	4.9	67	81	219.8
	20	5.1	58	74	460.6
	30	5.4	51	75	670.6
	35	5.0	50	77	805.4

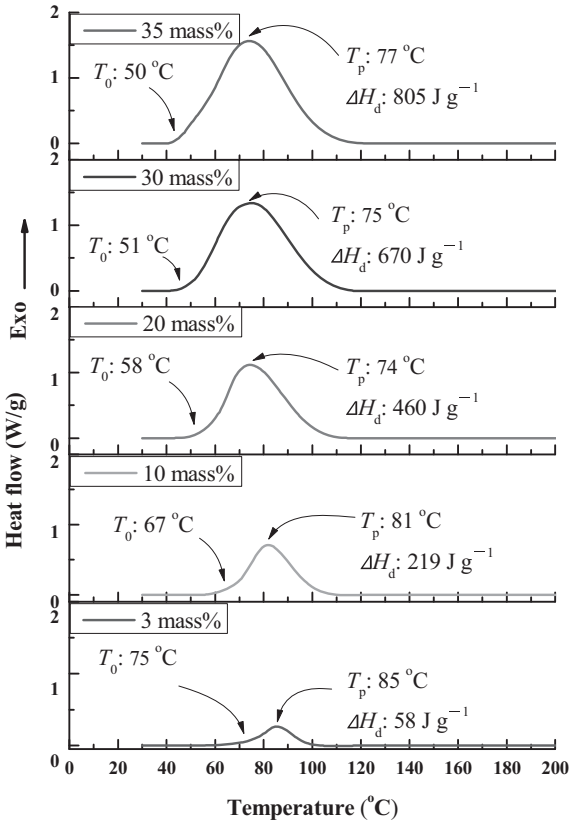

Figure 2. DSC thermal curves of heat flow versus temperature for H_2O_2 decomposition.

and 51 °C. After heating scanning, it could be stated that the phenomenon of T_0 of H_2O_2 was caused by the changes in exothermic temperature and released heat resulting from the different concentrations of H_2O_2 (3–30 wt %). The main interval of reaction temperature was measured from 50 °C to 80 °C concerning T_0 and T_p. Overall, after the catalytic decomposition of H_2O_2, a tremendous amount of heat would be generated.

To evaluate the thermal behavior of the mixing state for HPPO reaction, a uniform solution of 10 wt % H_2O_2, MeOH, and catalyst was sealed in the test cell under dynamic testing. The characteristics of thermokinetic parameters are presented in Tab. 2. Two main exothermic peaks appear at 50–120 °C and 190–250 °C, as illustrated in Fig. 3. The T_0 of first peak decreased from 67 °C to 50 °C during catalytic reaction when 10 wt % H_2O_2 was mixed with MeOH and catalyst. The main mechanism of the first phenomenon was that H_2O_2 had been

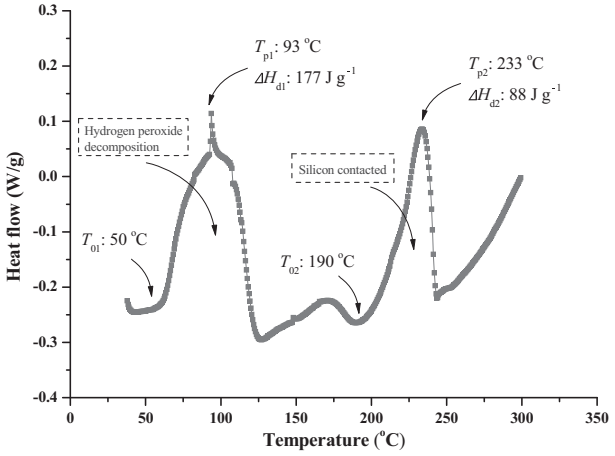

Figure 3. DSC thermal curves of heat flow versus temperature for the mixture of H_2O_2, MeOH, and catalyst under dynamic tests.

decomposed by a bivalent peroxide bond. The reaction temperature was similar with pure 10 wt % H_2O_2, as depicted in Fig. 2. Another one was ascribed to silicon contacting from the catalyst. In particular, the ΔH_d of the first peak was reduced by about 20 % from 219 to 177 J g^{-1}, for which the probable explanation was the unstable conversion of the solid catalyst during the parallel reaction for endothermic and exothermic states.

According to Fig. 2, the main purpose is to show the thermal curve of various concentrations for inherent safety in which the mass of H_2O_2 was around 5 mg. In this test, the ΔH_d of 10 wt % H_2O_2 was 219 J g^{-1}. In Fig. 3, the mass of 10 wt % H_2O_2 was around 3 mg and the curve was separated from H_2O_2 decomposition and silicon contacted. Therefore, the main reason for the drop in ΔH_d is that the lower mass of 10 wt % H_2O_2 was executed and the mechanism changed when H_2O_2 was mixed with MeOH and catalyst.

Moreover, past studies confirmed that organic peroxides (OPs) will be triggered to release enormous heat and gas under acidic or alkaline condition [22–24]. The pH-meter measured the pH value of the solution which contained MeOH and MeOH mixed with catalyst, respectively. The pH decreased from 6.76 to 4.37 when catalyst was uniformly stirred in MeOH (Fig. S1, Supporting Information). Obviously, it was easy to break the functional group, i.e., the oxygen–oxygen linkage for OPs during the process of HPPO reaction under acidic circumstances. Therefore, the adiabatic evaluation will be studied further after preliminary dynamic analyses by DSC.

Table 2. Experimental results for the mixture of H_2O_2, MeOH, and catalyst via DSC test at 4°C min^{-1}.

	Reactant		T_0 [°C]	T_p [°C]	ΔH_d [J g^{-1}]
Substance	Mass [%]	Mass [mg]			
H_2O_2	10	3			
MeOH	99	1.5	1st: 50 2nd: 190	1st: 93 2nd: 233	1st: 177 2nd: 88
Catalyst	–	1.5			

3.2 VSP2 Test Results: Adiabatic Hazard Analyses

H_2O_2 is defined as an explosive substance according to the National Fire Protection Association (NFPA 432). From Fig. 4 it follows that at 65 wt % H_2O_2 exothermic phenomena occur when the reaction is around 80°C. Because the temperature constantly and cumulatively increases, 5 g of the sample can result in a reaction temperature up to 235 °C under adiabatic conditions and a reaction pressure up to 608 psi.

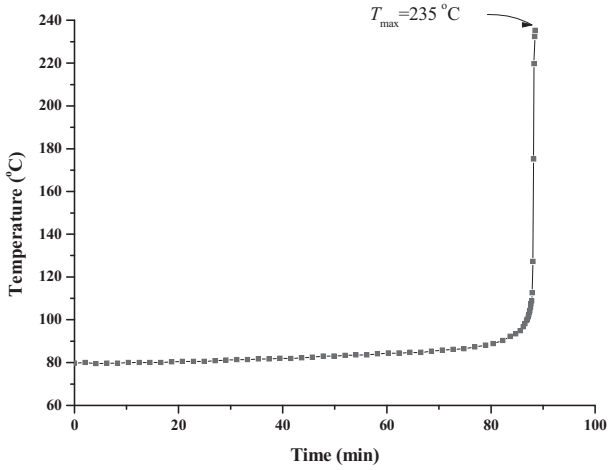

Figure 4. Temperature versus time curve with reactants for H_2O_2 by VSP2 test.

During runaway reactions, the temperature increases at a rate of 18 233 °C min^{-1} and the pressure increases at a rate of 76 116 psig min^{-1}, as indicated in Figs. 5–7. Physical data obtained from the thermal analysis are summarized in Tab. 3. These data suggest that when the reaction enters the phase of a non-reversible runaway reaction, the rates of the temperature increase and the pressure increase cannot be adequately resolved in time by an external cooling system or reaction neutralizer. At this moment, the withdrawal and evacuation of personnel is the most important response. The hazard data reveal

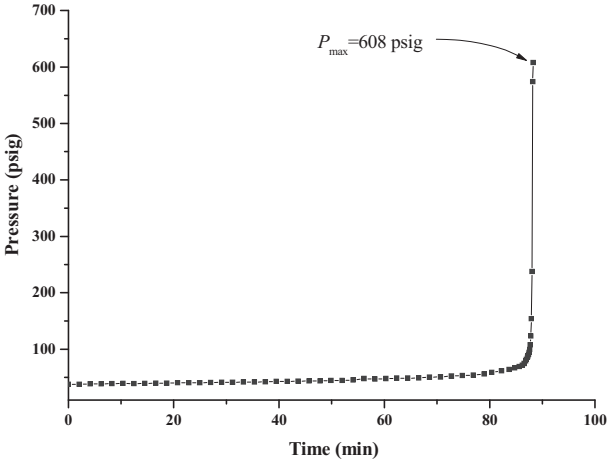

Figure 5. Pressure versus time curve with reactants for H_2O_2 by VSP2 test.

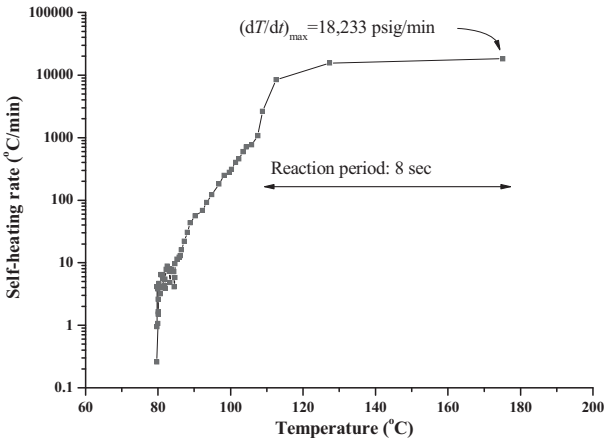

Figure 6. Self-heating rate versus temperature with reactants for H_2O_2 by VSP2 test.

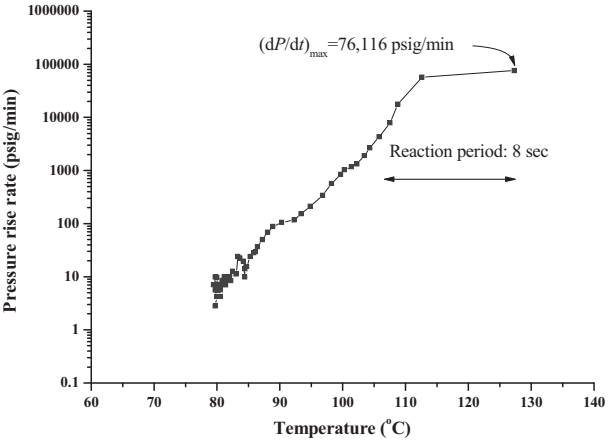

Figure 7. Pressure rise rate versus temperature with reactants for H_2O_2 by VSP2 test.

that the original H_2O_2 tank of the Taoyuan Yongxing resin plant had an H_2O_2 concentration of 50 % and weighed approximately 10 t. This tank was completely ruptured during this accident, which indicates the great power of the explosion [25].

To estimate the runaway characteristics under adiabatic condition, VSP2 was applied in the following experiment. For the real process, the specific ratio of MeOH and catalyst was uniformly mixed before being sealed in the VSP2 cell. Then propylene was added to keep the pressure at 24 psig and was continually maintained at the pre-set condition. After the system was treated at steady state, 35 wt % H_2O_2 was slowly injected to activate the HPPO reaction via high-pressure injector.

According to Fig. 8, the self-heating rate was about 0.1–0.3 °C min^{-1}, which means the HPPO was carried on at room temperature. The temperature started to increase rapidly and two peaks were generated after 40 °C. The first reaction time was 15 min and T_{max} was 189 °C; the second reaction time and T_{max} were 43 min and 191 °C, respectively.

Fig. 9 shows the relationship between reaction time and pressure. The fluctuations at the beginning were caused by the injection of propylene. When the reaction temperature started to

Table 3. Parameters of runaway characteristics for H_2O_2 with various reactants by VSP2.

	Reactant		T_0 [°C]	T_{max} [°C]	P_{max} [psig]	$(dT/dt)_{max}$ [°C min^{-1}]	$(dP/dt)_{max}$ [psig min^{-1}]
	Material	Mass [g]					
Inherent hazard analyses	65 wt % H_2O_2	5	74	235	608	18 233	76 116
	35 wt % H_2O_2	0.60	40	191.0	474.0	27.3	90.2
HPPO reaction	MeOH	10.2					
	Catalyst	0.12					
	Propylene	–					

increase, after a short reaction time the pressure started to grow and two pressure peaks were produced. The first maximum pressure (P_{max}) was 121.4 psig and the second one was 86.8 psig.

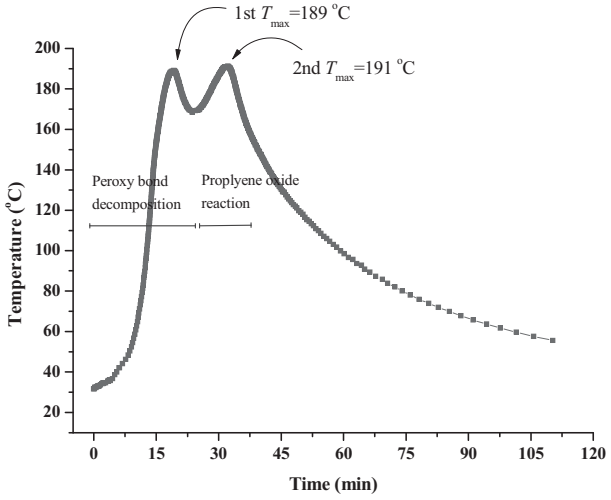

Figure 8. Temperature versus time curve with reactants for HPPO reaction by VSP2 test.

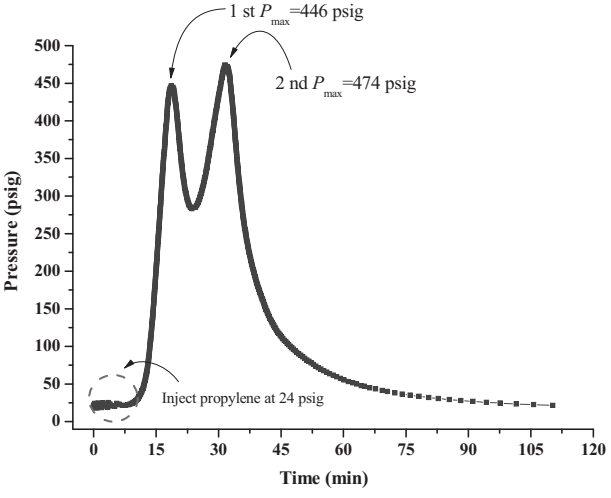

Figure 9. Pressure versus time curve with reactants for HPPO reaction by VSP2 test.

Figs. 10 and 11 compare between reaction temperature and heating rate and between reaction temperature and pressure rise rate. It was found that $(dT/dt)_{max}$ was 18.2 °C min^{-1} and $(dP/dt)_{max}$ was 23.2 psig min^{-1}. Overall, the first peak arose related to H_2O_2 for which the exothermic temperature was in line with the DSC test. The second peak occurred due to the HPPO reaction with propylene, MeOH, and catalyst.

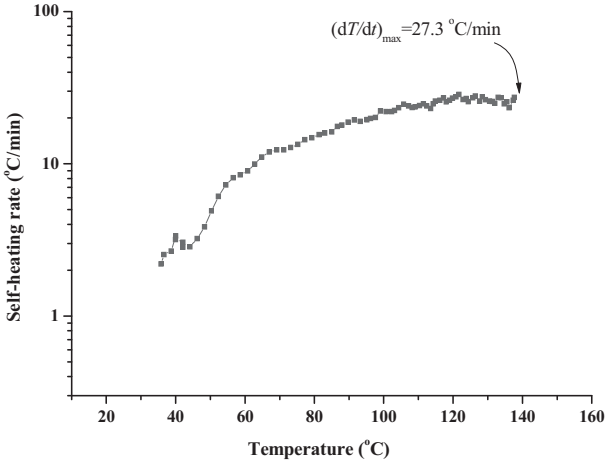

Figure 10. Self-heating rate versus temperature with reactants for HPPO reaction by VSP2 test.

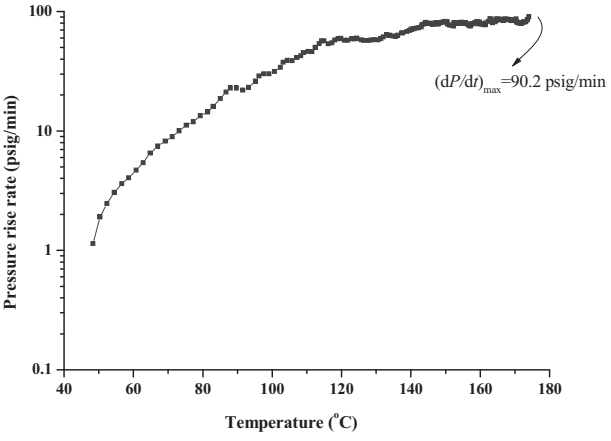

Figure 11. Pressure rise rate versus temperature with reactants for HPPO reaction by VSP2 test.

The changes in the pressure were beyond the originally expected magnitude. Tab. 3 lists the thermodynamic data using VSP2 obtained from the tests. Even though the $(dT/dt)_{max}$ and $(dP/dt)_{max}$ were not violent, the scale of temperature under the adiabatic conditions was about 150 ± 10 °C from room temperature. The instability origin of these peroxides from H_2O_2 lies in the specific oxygene–oxygen linkage, which is known for its weak energy, i.e., 80–200 kJ mol^{-1} [25]. The thermal hazard generated after the injection of propylene in the evenly mixed MeOH, catalyst, and H_2O_2 was verified in order to prevent losses resulting from a runaway reaction and to reduce the frequency of thermal disasters that may occur.

3.3 Thermal Hazard of Temperature Variation Equation

Based on the worst-case thermal hazard scenario, the 35 wt % H_2O_2 and HPPO reaction (35 wt % H_2O_2, propylene, MeOH, catalyst) were selected from the series of VSP2 tests. The models are mainly described in this study by Eqs. (1)–(11). Thermokinetic parameters could be obtained to define the degree of hazard during the exothermic reaction.

In the VSP2 test, heat generated by thermal decomposition of a sample is also employed to heat the test cell, so it is necessary to consider the thermal inertia factor. The energy balance equation of the adiabatic reaction system is:

$$\varphi m C_v \frac{dT}{dt} = (-\Delta H) r V \tag{1}$$

where the thermal inertia factor is defined as:

$$\varphi \equiv \frac{m_s C_v + m_R C_{vR}}{m_s C_v} \tag{2}$$

The reaction rate equation is expressed as:

$$r = -\frac{dC}{dt} \tag{3}$$

The above equation is substituted into Eq. (1) and integrated from initial temperature and concentration to final temperature. Here, zero concentration is under the assumption of $-\Delta H$, Φ, ρ, and C_v to be constant:

$$\frac{-\Delta H}{\varphi \rho C_v} = \frac{T_f - T_0}{C_0} \tag{4}$$

and

$$\frac{dT}{dt} = \frac{T_f - T_0}{C_0}\left(-\frac{dC}{dt}\right) \tag{5}$$

The adequate concentration–temperature relationship can be obtained by integrating the above equation, being approximately:

$$\frac{C}{C_0} = \frac{T_f - T}{T_f - T_0} \tag{6}$$

For a single *n*th-order reaction:

$$r = -\frac{dC}{dT} = kC^n \tag{7}$$

with

$$k = k_0 e^{\frac{-E_a}{RT}} \tag{8}$$

The self-heating rate is obtained from Eqs. (5)–(8):

$$\frac{dT}{dt} = \left(\frac{T_f - T_0}{C_0}\right) k C_0^n \left(\frac{T_f - T}{T_f - T_0}\right)^n = k\left(\frac{T_f - T}{T_f - T_0}\right)^n (T_f - T_0) C_0^{n-1} \tag{9}$$

so:

$$k = \frac{dT/dt}{C_0^{n-1}\left(\frac{T_f - T}{T_f - T_0}\right)^n (T_f - T_0)} \tag{10}$$

From Eqs. (9) and (10) it follows:

$$\ln k = \ln k_0 - \frac{E_a}{RT} = \ln \frac{dT/dt}{C_0^{n-1}\left(\frac{T_f - T}{T_f - T_0}\right)^n (T_f - T_0)} \tag{11}$$

Eq. (11) could be used to acquire the frequency factor k_0 and the activation energy E_a at the same time [26]. According to Eq. (11), selecting a proper reaction order *n*, it is a valid method to obtain the thermokinetic parameters and to operate the thermal hazard prediction from adiabatic tests. First, the linear analysis results by $\ln((dT/dt)/(T_f-T))$ vs. $1/T$ were applied to obtain the E_a and k_0. The calculated results are depicted in Figs. 12 and 13, and the calculated thermokinetic parameters are presented in Tab. 4 for the purpose of simulating experimental data and thermal hazard prediction.

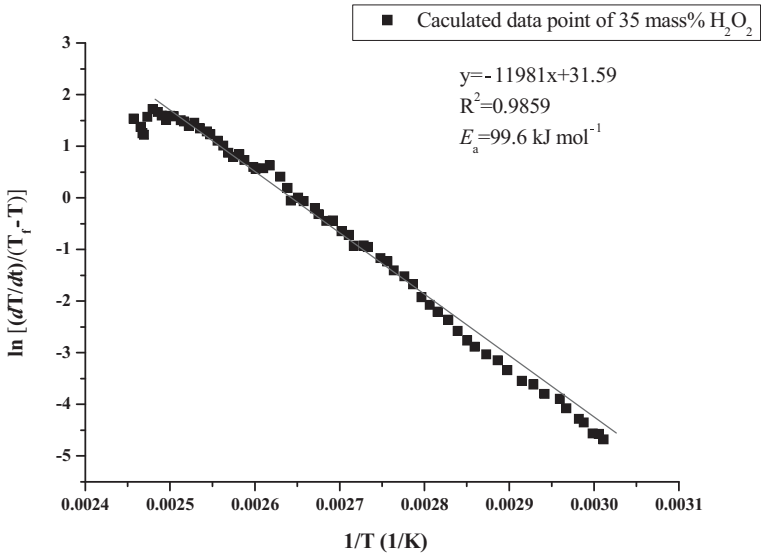

Figure 12. Estimation of the thermokinetic parameters of 35 wt % H_2O_2 from experimental data of VSP2.

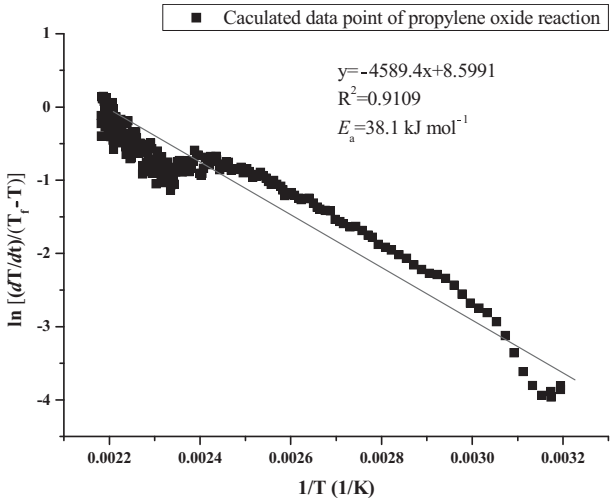

Figure 13. Estimation of the thermokinetic parameters of HPPO reaction from experimental data of VSP2.

Table 4. Thermokinetic parameters for 35 wt % H_2O_2 and HPPO reaction from VSP2 test via temperature variation equation.

Component	E_a [kJ mol^{-1}]	k_0 [mol L^{-1}s^{-1}]
35 wt % H_2O_2	99.6	5.24×10^{13}
HPPO reaction	38.1	5426

After calculation, the E_a of 35 wt % H_2O_2 and HPPO reaction were 99.6 and 38.1 kJ mol^{-1} and k_0 were 5.24×10^{13} and 5.426×10^3, respectively. The results show that the HPPO reaction is going on more easily than pure H_2O_2 with lower E_a. The phenomenon agreed with the VSP2 test in which T_0 was 40 °C for thermal decomposition. Admittedly, the lower E_a could be a proper situation for the reactor that the reaction rate changes fast to start the chain reaction without amount of heat energy. However, the lower the E_a existing in the process, the higher is the degree of disaster that may potentially occur. In view of inherent safety, the potential hazard should be controlled via VSP2 test and temperature variation equation to evaluate various parameters.

As a result, the system pressure can increase, and thermal runaway or explosions may occur. Data obtained from adiabatic curves can be used to assess the hazards of HPPO reaction and the potential for thermal runaway. In the present study, the potential for thermal runaway in the HPPO reaction was confirmed and the hazards of H_2O_2 were determined.

4 Conclusions

The effect of the runaway reaction of HPPO reaction in the presence of H_2O_2 was evaluated using DSC and VSP2 by dynamic and adiabatic methods, according to the thermal decomposition of the catalytic reaction of various tests as well as thermal curves and the experimental data acquired from the research results. In the actual manufacturing process, in addition to the high reactivity of H_2O_2, the content of propylene may become a key substance, resulting in runaway excursions. Thus, with the results of the present study, the process safety specialist can determine the amount of time needed before corrective actions must be performed and the appropriate course of action in hazardous situations should be taken.

Acknowledgment

Financial support from the China Petrochemical Development Corporation (CPDC) in Taiwan is gratefully acknowledged.

The authors have declared no conflict of interest.

Symbols used

C_v	[mol L^{-1}]	heat capacity of the sample under constant volume per mass
C_{vR}	[mol L^{-1}]	heat capacity of the reactor or vessel under constant volume per mass
E_a	[kJ mol^{-1}]	apparent activation energy
ΔH_d	[J g^{-1}]	heat of decomposition
m_R	[g]	mass of the reactor vessel
m_S	[g]	mass of the sample
P	[psig]	pressure
P_{max}	[psig]	maximum pressure
$(dP/dt)_{max}$	[psig min^{-1}]	maximum pressure rise
R	[J K^{-1}mol^{-1}]	ideal gas law constant
T	[°C]	temperature
T_0	[°C]	exothermic onset temperature
T_{max}	[°C]	maximum temperature
T_p	[°C]	exothermic peak temperature
$(dT/dt)_{max}$	[°C min^{-1}]	maximum temperature rise
t	[min]	time

Greek letters

Φ	[–]	thermal inertia

Abbreviation

HPPO	propylene oxide

References

[1] H. Y. Hou, C. H. Su, C. M. Shu, *J. Loss Prev. Process Ind.* **2012**, *48*, 176–180.
[2] H. Y. Hou, C. M. Shu, Y. S. Duh, *AIChE J.* **2001**, *47*, 1893–1896.
[3] J. Schmidt, S. Egan, *Chem. Eng. Technol.* **2009**, *32*, 263–272.
[4] J. Jiang, J. Jiang, Y. Pan, R. Wang, P. Tang, *Chem. Eng. Technol.* **2011**, *34*, 1521–1528.
[5] G. F. Thiele, E. Roland, *J. Mol. Catal. A: Chem.* **1997**, *117*, 351–356.
[6] J. M. Tseng, C. M. Shu, Y. C. Yu, *Korean J. Chem. Eng.* **2005**, *22*, 797–802.

[7] M. G. Clerici, G. Bellussi, U. Romano, *J. Catal.* **1991**, *129*, 159–167.
[8] S. H. Liu, H. Y. Hou, J. W. Chen, S. Y. Weng, Y. C. Lin, C. M. Shu, *Thermochim. Acta* **2013**, *566*, 226–232.
[9] C. Y. Jhu, Y. W. Wang, C. Y. Wen, C. M. Shu, *Appl. Energy* **2012**, *100*, 127–131.
[10] W. T. Chen, C. C. Ma, M. H. Lee, Y. C. Chu, L. C. Tsai, C. M. Shu, *Appl. Energy* **2012**, *100*, 187–192.
[11] Y. T. Tsai, M. L. You, X. M. Qian, C. M. Shu, *Ind. Eng. Chem. Res.* **2013**, *52*, 8206–8215.
[12] F. C. Tsai, N. Ma, L. C. Tsai, J. Tao, T. C. Chiang, Y. C. Chu, W. T. Chen, C. M. Shu, *Energy Educ. Sci. Technol. Part A* **2012**, *30*, 1137–1142.
[13] T. S. Wang, S. H. Liu, X. M. Qian, C. M. Shu, *J. Therm. Anal. Calorim.* **2013**, *113*, 1625–1631.
[14] T. A. Nijhuis, M. Makkee, J. A. Moulijn, B. M. Weckhuysen, *Ind. Eng. Chem. Res.* **2006**, *45*, 3447–3459.
[15] A. Wróblewska, E. Lawro, E. Milchert, *Ind. Eng. Chem. Res.* **2006**, *45*, 7365–7373.
[16] J. M. Man, Q. D. Zhang, H. J. Xie, J. X. Pan, Y. S. Tan, Y. Z. Han, *J. Fuel Chem. Technol.* **2011**, *39*, 42–46.
[17] M. Ghanta, D. R. Fahey, D. H. Busch, B. Subramaniam, *ACS Sustainable Chem. Eng.* **2013**, *1*, 268–277.
[18] Mettler Toledo, *STAR^e Thermal Analysis*, Sweden **2013**.
[19] Y. W. Wang, Y. S. Duh, C. M. Shu, *Ind. Eng. Chem. Res.* **2001**, *40*, 1125–1132.
[20] C. C. Huang, J. J. Peng, S. H. Wu, H. Y. Hou, M. L. You, C. M. Shu, *J. Therm. Anal. Calorim.* **2010**, *102*, 579–585.
[21] L. C. Tsai, J. W. Chen, H. Y. Hou, S. H. Liu, C. M. Shu, *J. Therm. Anal. Calorim.* **2012**, *109*, 1303–1309.
[22] J. H. Chi, S. H. Wu, J. C. Charpentier, Y. P. I, C. M. Shu, *J. Loss Prev. Process Ind.* **2012**, *25*, 142–147.
[23] S. H. Wu, J. H. Chi, C. C. Huang, N. K. Lin, J. J. Peng, C. M. Shu, *J. Therm. Anal. Calorim.* **2010**, *102*, 563–568.
[24] H. Y. Hou, Y. S. Duh, W. L. Lee, C. M. Shu, *J. Therm. Anal. Calorim.* **2009**, *2*, 541–545.
[25] J. H. Chi, S. H. Wu, J. C. Charpentier, Y. P. I, C. M. Shu, *J. Loss Prev. Process Ind.* **2012**, *25*, 142–147.
[26] H. J. Liaw, C. C. Yur, Y. F. Lin, *J. Loss Prev. Process Ind.* **2000**, *13*, 499–507.

